RSC Advances

ROYAL SOCIETY OF CHEMISTRY

www.rsc.org/advances

Journal Name

ARTICLE

Toughening of Amorphous Poly(propylene carbonate) by Rubbery CO_2-based Polyurethane: Transition from Brittle to Ductile

Received 00th January 20xx,
Accepted 00th January 20xx

DOI: 10.1039/x0xx00000x

www.rsc.org/

Guanjie Ren[ab], Yuyang Miao[a], lijun Qiao[a], Yusheng Qin[*a], Xianhong Wang[**a], Fosong Wang[a]

Amorphous poly (propylene carbonate) (PPC) is brittle at room temperature, toughening of PPC is hardly realized. Here two kinds of polyurethane (PCO_2PU) synthesized from CO_2-based diol and toluene diisocyanate were used as rubbery particle to toughen PPC. The notched impact strength of PPC increased suddenly from 20.8 J/m to 54.2 J/m at PCO_2PU loading of 20 wt%, comparable with that of neat nylon 6, and reached 228.3 J/m at PCO_2PU loading of 30 wt%, 10.9 folds of neat PPC, even higher than bisphenol A polycarbonate. The matrix yielding as well as cavitation was observed during the impact process, which was responsible for the increase of impact strength. Meanwhile, the toughening efficiency related with the carbonate content of PCO_2PU, and transition of fracture behavior from brittle to ductile occurred when the PCO_2PU dispersed in PPC substrate uniformly with weight average diameter of 0.20 μm.

Introduction

Poly (propylene carbonate) (PPC) is an alternative copolymer of CO_2 and propylene oxide, it has received much attention in the past decades, since it is biodegradable in addition to effective CO_2 utilization.[1] Now it has found applications not only in high value-added area like tissue scaffolds[2] or polymer electrolyte,[3] but also in low cost biodegradable packaging material.[4] However, PPC is amorphous and brittle with elongation at break below 10% and low notched impact strength of about 20 J/m at 20 °C, which is comparable to polystyrene with notched impact strength of 15.8 J/m. Generally, the notched impact strengths of high density polyethylene (HDPE) and high impact strength polystyrene (HIPS) were 50-70 J/m[5] and 72-148 J/m,[6] respectively. Therefore, the notched impact strength of PPC is quite low, which has severely limited its application.

Much effort has been made to overcome the brittleness of PPC, our effort indicates that PPC can be plasticized by diallyl phthalate[7] or low molecular weight urethane compound,[8] or partly plasticized and enhanced by introducing hydro-branched poly(ester amide) via hydrogen bonding interaction.[9] The elongation at break has been improved to over 700% while a completely miscible blend has been obtained,[8] however, currently no report has been related to the notched impact test, while it represents the ability to absorb fracture energy under high loading in a notched state.

The notched impact strength of general polymer like polyamide[10] or polystyrene[11] has been investigated for a long time. The introduction of elastomer (with appropriate domain size or interparticle distance) into the matrix can change the stress state around the particles and form microstructures dissipating impact energy, such as intensified stable crazing in HIPS[11b, 11c] and large area of shear yielding[10b, 10c] accompanying cavitation in polyamide.[10a, 10d, 10e] Both the notched impact strength and fracture morphology are significantly related to the rubber particle diameter and the volume fraction,[12] and raising the content of small rubber particles favors local plane stress with the consequence of transition from crazing to shear deformation. For a given polymer blend, maximum toughness can be obtained in a limited range of rubber particle size,[12b] where microvoid is formed avoiding the premature of fracture due to the extension of craze from the notch tip before significant energy has been dissipated, which facilitates the occurrence of shear yielding. For example, in a polyamide/polyolefin elastomer blend,[12a] energy dissipated by shear yielding reached optimum at particle size between 0.1 μm and 0.3 μm.

The CO_2-based polyurethane (PCO_2PU) (Scheme1) was synthesized from chain extending reaction of CO_2-based diols with toluene diisocyanate (TDI), it shows rubbery. The CO_2-based diol with different molecular weight and carbonate content was prepared in this lab by the copolymerization of propylene oxide and CO_2,[13] which has low molecular weight (number average molecular weight of *Ca.*1,000-1,500g/mol) and perfect OH functionality. It is noteworthy that such CO_2-based diol has 20-30% lower cost than conventional polypropylene glycol (PPG), it may be a competitive raw material for polyurethane formation. Most importantly, the existence of similar carbonate unit between the PCO_2PU and PPC may enhance the miscibility of the two components. Also

[a]*Address here.*
[b]*Address here.*
[c]*Address here.*
† Footnotes relating to the title and/or authors should appear here.
Electronic Supplementary Information (ESI) available: [details of any supplementary information available should be included here]. See DOI: 10.1039/x0xx00000x

bonus may come from the formation of intermolecular hydrogen bonding between N-H in the main chain of PCO_2PU and carbonyl group in PPC. Therefore, two kinds of rubbery PCO_2PU with different carbonate content were used to toughen PPC, a sudden increase of notched impact strength to the value of neat polyamide (PA6) was observed accompanying the fracture behavior transition from brittle to ductile, and matrix shear yielding appeared for the domain size of PCO_2PU at 0.20 μm.

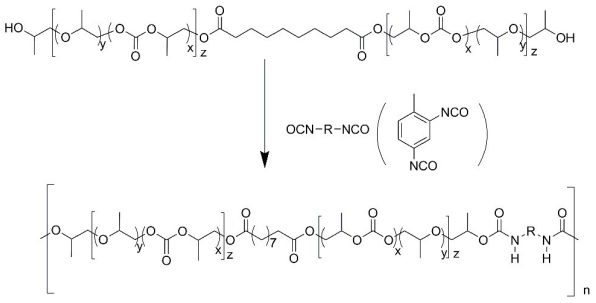

Scheme1. Synthesize of PCO_2PU with CO_2-based diol

2. Experiment

2.1 Materials

Toluene diisocyanate (TDI) and dibutyltin dilaurate were purchased from Tianjin Guangfu chemical Research Institute (China) and used as received. The CO_2-based diols with carbonate unit content of 50.4% and 62.3% was prepared by our laboratory according to the literature.[13] The number-average molecular weight (M_n) of CO_2-based diol with 50.4% carbonate unit content was 1,377 $gmol^{-1}$. The number-average molecular weight (M_n) of CO_2-based diol with 62.3% carbonate unit content was 1,245 $gmol^{-1}$.

PPC was supplied by Zhejiang Bangfeng Plastic *Co.* (China), whose technique was licensed under our laboratory. To remove residue rare earth metal ternary catalyst, the copolymer was purified twice by repeated dissolution/precipitation procedure with dimethyl carbonate as a solvent and ethanol as a precipitate. The number-average molecular weight (M_n) and the polydispersity index (PDI) of the purified PPC were determined by gel permeation chromatography (GPC) as 17.3×10^4 g/mol and 3.65, respectively. The carbonate unit content of the purified PPC was 92%, estimated from its ^{1}H NMR spectrum according to the literature.[14]

2.2 Synthesis of PCO_2PUs

PCO_2PU was synthesized by the polyaddition of CO_2-based diols and TDI under N_2 protection. Briefly, CO_2-based diols (0.035 mol) were dried at 80 °C under vacuum for 40 min to complete dehydration. TDI (0.035 mol) and dibutyltin dilaurate (3.0 μL) were injected into the reaction vessel and stirred at 110 °C for 30 min. The resultant PCO_2PUs from CO_2-based diol with 50.3% and 62.4% carbonate unit were denoted as PCO_2PU1, PCO_2PU2, respectively. The ^{1}H NMR (d_6-$CHCl_3$, TMS, 300MHz) data were listed as follows.

PCO_2PU1: δ (ppm) = 7.61, 7.21, 7.07 (-ArH), 5.17-4.76 (-$CH_2CH(CH_3)OCOO$-), 3.97-4.34 (-$CH_2CH(CH_3)OCOO$-), 3.25-3.81 (-$CH_2CH(CH_3)O$-), 2.30 (-CH_2COO-), 2.20 (-$ArCH_3$), 1.29 (-$CH_2CH(CH_3)OCOO$-, -$CH_2CH_2CH_2CH_2COO$-), 1.14 (-$CH_2CH(CH_3)O$-)

PCO_2PU2: δ (ppm) = 7.67, 7.20, 7.06 (-ArH), 5.20-4.78 (-$CH_2CH(CH_3)OCOO$-), 3.93-4.36 (-$CH_2CH(CH_3)OCOO$-), 3.30-3.88 (-$CH_2CH(CH_3)O$-), 2.30 (-CH_2COO-), 2.20 (-$ArCH_3$), 1.28 (-$CH_2CH(CH_3)OCOO$-, -$CH_2CH_2CH_2CH_2COO$-), 1.16 (-$CH_2CH(CH_3)O$-)

2.3 Melt-blending procedure

Prior to the blending, PPC and PCO_2PUs were dried at 45 °C in vacuum for 24 h. Then PPC and PCO_2PU were mixed in calculated weight ratio (PCO_2PU/PPC = 2.5/97.5, 5/95, 10/90, 15/85, 20/80, 30/70). The mixing was operated on a Haake batch-intensive mixer (Haake Rheomix 600) at a speed of 60 r/min for 5 min at 140 °C. All the blends were kept in a desiccator before use.

2.4 Characterization

Tensile performance was evaluated using dumb-bell-shaped sample punched out from the molded sheet in a screw-driven universal testing machine (Z010, Zwick Co., Germany) equipped with a 10 kN electronic load cell and mechanical grips. The test was conducted at 20 °C using a cross-head rate of 20 mm/min according to the ASTM standard, and the data reported were the mean of the parallel values in five determinations.

The Izod notched impact strength of the specimens was carried out on a JJ-20 instrumented impact machine at 20 °C according to the ASTM D256-04. At least five specimens were tested for each sample to get an average value.

Scanning electron microscopy (SEM) experiments were performed using XL30 ESEM FEG (FEI Co.) instrument with an acceleration voltage of 8 KV. The fracture surfaces of Izod notched impact test were coated with gold to increase the contrast.

Differential scanning calorimetry (DSC) analysis was performed on a Perkin-Elmer DSC-7 instrument under N2 atmosphere. The sample was first heated from -50 °C to 50 °C at 10 °C/min and then rapidly quenched to -50 °C, followed by second heating process to obtain the glass transition temperature (T_g) to eliminate the thermal history.

Rheological measurements were performed at 140 °C using a AR 2000 (TA, USA) rheometer with a parallel plate geometry and 25 mm plate diameters. Dynamic amplitude sweeps from 0.1 to 100% strain at 1 rad/s frequency were executed to determine the linear viscoelasticity range. Then dynamic frequency sweeps were performed from 0.01 to 100 rad/s at a small strain of 1% within the linear viscoelastic zone.

The TEM images were recorded on a transmission electron microscope (Tecnai G2 F20 S-TWIN) with acceleration voltage of 200 kV. The samples for TEM analysis were prepared by microtoming 50-100 nm thickness films from the blends with an ultramicrotome (LEICA ULTR CUTR ME1-057) and stained with 1% aqueous phosphotungstic acid. The rubber particle size from the TEM was calculated using Nanomeasure

software. The number and weight average rubber particle sizes were calculated using the following equations.

$$\overline{d_n} = \frac{\sum n_i d_i}{\sum n_i}$$

$$\overline{d_w} = \frac{\sum n_i d_i^2}{\sum n_i d_i}$$

3. Results and discussion

3.1 Tensile properties and impact strength

The stress-strain curves of PPC/PCO_2PU blends were plotted in Fig. 1, the corresponding parameters were listed in Table 1. Neat PPC displayed brittle fracture with elongation at break of 9.83%, it increased to 28.74% when the loading of PCO_2PU1 reached 5 wt%. It was noteworthy that both the tensile strength and the modulus of the blend with 5 wt% PCO_2PU1 increased by 10.21 MPa and 89.48 MPa compared with those of neat PPC, respectively. Further increasing the PCO_2PU1 loading to 20 wt%, the elongation at break increased to 49.83% while the tensile strength still remained 47.66 MPa. When the loading of PCO_2PU1 increased to 30 wt%, the elongation at break reached 320.76% with the tensile strength decreasing to 27.36MPa. Similar toughening effect can be observed in PPC/PCO_2PU2 blends. When the PCO_2PU2 loading was 20 wt%, the elongation at break increased to 33.06% while the tensile strength was still 4.32 MPa higher than that of the neat PPC. Therefore, simultaneous increase of the tensile strength and elongation at break was realized in this polyblending system, especially at relative low PCO_2PU loading, which may be related to the intermolecular hydrogen bonding between the C=O of PPC and the NH of PCO_2PU, as reported in PLA/Hyperbranched Polyamide blend[15] and PPC/low-molecular weight urethane blend.[8] It was common that addition of rubbery particle toughened the matrix while decreased the tensile strength. But the existence of hydrogen bonds can enhance the interfacial adhesion and improve the tensile strength.[9] Therefore, the tensile strength of the blend increased with PCO_2PU1 loading below 15 wt%, when the PCO_2PU1 loading was above 15 wt%, the stereo hindrance and dilution effect became dominant suppressing the reinforcing effect of PCO_2PU. Compared with PCO_2PU1, PCO_2PU2 with higher carbonate content showed more significant reinforcing effect, which may be related to the content of hydrogen bonded C=O in PPC. Meanwhile, it seemed that the PCO_2PU1 was more effective than PCO_2PU2 in toughening PPC, therefore, the impact test was conducted to confirm the toughening effect.

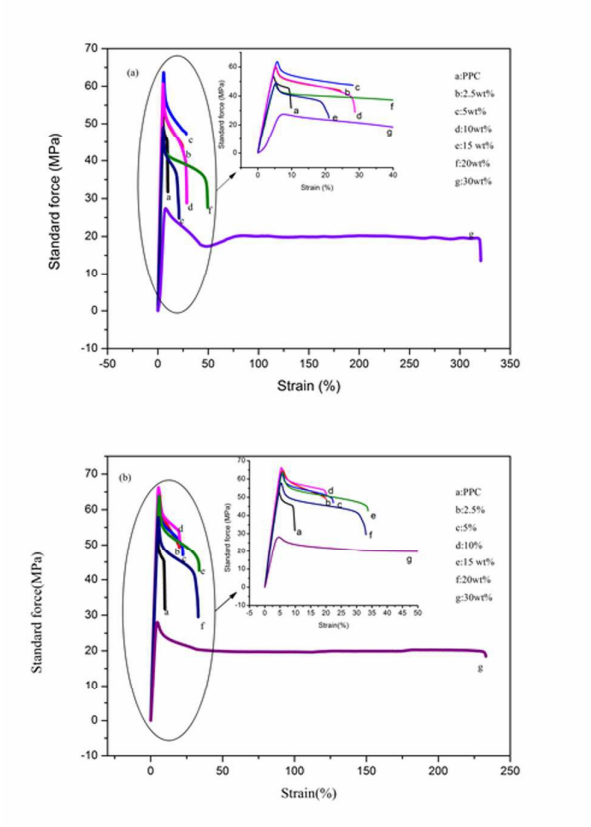

Fig. 1. Stress-strain curves of PPC/PCO_2PU1 (a) and PPC/PCO_2PU2 (b)

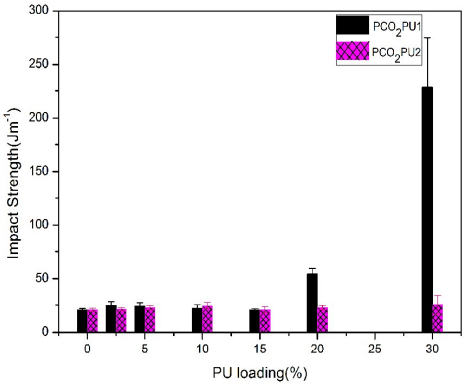

Fig. 2. Notched impact strengths of PPC/PCO2PUs with various PCO2PU loadings

The notched impact strengths of PPC/PCO_2PU blends were displayed in Table 2 and Fig. 2. When the PCO_2PU1 loading was below 20 wt%, the notched impact strength increased few and it increased suddenly by 33.4 J/m from 20.8 J/m to 54.2 J/m with PCO_2PU1 loading increased to 20 wt%. Further increasing the PCO_2PU1 loading to 30wt%, the notched impact strength increased to 228.3 J/m. PCO_2PU2 showed nearly no toughening effect in all range of composition studied. The PCO_2PU1 was more effective in toughening PPC, which was more obvious in the notched impact test.

It is reasonable that the elongation at break of PPC/PCO_2PU2 blends increased significantly while the notched impact strength was improved few, for the notched impact strength was more accurate. As far as the PPC/PCO_2PU1 blend was concerned, the PCO_2PU1 toughened PPC effectively at 20 wt% loading and the notched impact strength was comparable with that of neat PA6.[16] With increasing loading to 30 wt%, although

the tensile strength decreased to 27.36 MPa, the notched impact strength increased to 10.9 folds of neat PPC, which was even higher than the bisphenol A polycarbonate.[17]

The improved notched impact strength may indicate occurrence of brittle-ductile transition, which may be accompanied by the formation of microstructure such as shear yielding, crazes and microvoids. To confirm the microstructure formed during the impact test and understand the toughening mechanism, the fracture surfaces of neat PPC and PPC/ PCO_2PU blends under the loading of 20 wt% and 30 wt% were studied in the following.

Table 1 Main mechanical properties of PPC/PCO_2PU with various PCO_2PU loading

Sample	PCO_2PU ratio (wt%)	Young's modulus(MPa)	Tensile strength(MPa)	Elongation at break(%)
PPC/ PCO_2PU1	0	1392.91±60.84	53.47±2.48	9.83±5.28
PPC/ PCO_2PU1	2.5	1407.07±51.74	59.83±3.13	24.60±9.32
PPC/ PCO_2PU1	5	1482.39±67.85	63.68±3.31	28.74±5.07
PPC/ PCO_2PU1	10	1420.6±134.29	60.69±4.85	28.71±4.17
PPC/ PCO_2PU1	15	1144.66±79.13	49.01±3.04	21.02±5.28
PPC/ PCO_2PU1	20	1086.76±126.49	47.66±1.90	49.48±7.53
PPC/PCO_2PU1	30	680.05±109.49	27.36±1.40	320.76±51.44
PPC/ PCO_2PU2	2.5	1424.79±72.52	61.99±3.39	21.97±4.96
PPC/ PCO_2PU2	5	1449.79±67.56	63.28±2.89	22.37±4.96
PPC/ PCO_2PU2	10	1474.11±25.50	66.23±1.79	20.22±4.59
PPC/ PCO_2PU2	15	1323.54±48.24	63.78±2.72	33.74±6.31
PPC/ PCO_2PU2	20	1164.90±40.76	57.79±2.96	33.06±5.15
PPC/PCO_2PU2	30	730.59±109.01	28.03±1.44	233.01±49.70

Table 2 Notched impact strengths of PPC/PCO_2PUs with various PCO_2PU loadings

Sample	0	2.5 wt%	5 wt%	10 wt%	15 wt%	20 wt%	30wt%
PPC/PCO_2PU1 (J m-1)	20.8±1.4	24.7±3.2	24.2±2.9	22.2±3.2	20.5±1.3	54.2±5.1	228.3±46.3
PPC/PCO_2PU2 (J m-1)	20.8±1.4	21.3±1.6	22.7±2.1	24.7±3.1	20.8±3.1	22.8±2.1	25.5±8.6

3.2 Toughening mechanism

SEM images on fracture surface of PPC and the polyblends were shown in Fig. 3. In Fig. 3a, the fracture surface of neat PPC was a typical brittle appearance, it was relatively smooth with ellipse mark, indicating that the secondary-crack-front velocity was bigger than that of main-crack-front.[18] When PPC was blended with 20 wt% PCO_2PU1, the corresponding fracture surface showed no ellipse mark and became coarser with matrix shear yielding appeared (Fig. 3c). Meanwhile, a few cavitations can be found in the magnified image (Fig. 3d). At 30 wt% PCO_2PU1 loading, large area of shear yielding with cavitation was observed, and the fracture surface showed typical ductile appearance (Fig. 3e). Compared with PCO_2PU1, the addition of 20 wt% and 30 wt% PCO_2PU2 did not change much the fracture surface of PPC, and no cavitation and massive shear yielding can be observed, correponding to the few increase of impact strength of PPC/PCO_2PU2 (Fig. 3g and Fig. 3i).

It has been reported that for polyblends showing massive shear yielding in the matrix upon impacting, most energy will be dissipated from the matrix yielding.[19] Though the formation of microvoids is the secondary factor contributing to toughening, it is necessary in the formation of massive shear yielding. The cavitation reduces the critical stress at the onset of shear yielding to avoid obtaining the critical strain energy release rate first.[12b] In the PPC/PCO_2PU1 blends with 20 wt% PCO_2PU1, cavitation as well as shear yielding was obseved, indicating a transiton from brittle to ductile occurred, and the impact strength increased. However, the absence of massive cavitation determined the shear yielding was not as massive as that observed in PLA blend[20] or in PP blend.[21] At 30 wt% PCO_2PU1 loading, the cavitation as well as the shear yielding was expanded to the whole range and the impact strength was improved largely. Therefore, the cavitation and shear yielding resulted in the increase of notched impact strength. In addition, the occurrence of cavitation and shear yielding in the PPC/PCO_2PU1 blends at the loading of 20 wt% may be relate to the morphology of the blend. Therefore, the miscibility and morphology were studied in the following.

3.3 DSC analysis of various PPC/PCO_2PU blends

To study the miscibility between PPC and two kinds of PCO_2PU, the DSC curves of PPC/PCO_2PU1, PPC/PCO_2PU2 with various compositions were recorded in Fig. 4. There was only single glass transition temperature at low loading of PCO_2PU for all the blends, suggesting good miscibility between PPC and PCO_2PU at the loading below 5 wt%. However, another glass transition temperature appeared when PCO_2PU loading was above 5 wt%, indicating the occurrence

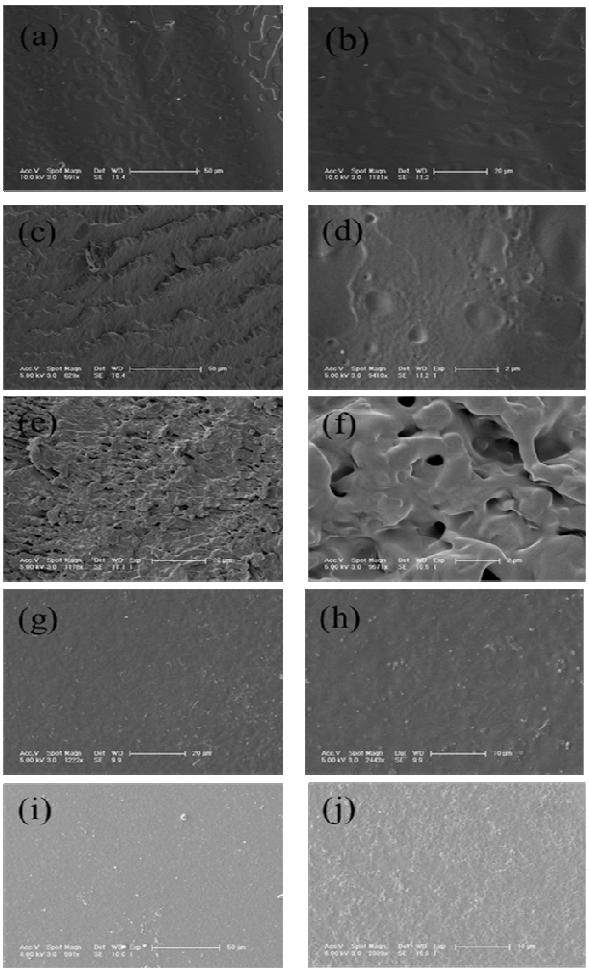

Fig. 3. SEM images of fracture surface of PPC/PCO_2PU impact sample: (a,b) PPC, (c,d) PPC/PCO_2 PU1(80/20), (e,f) PPC/PCO_2PU1 (80/30), (g,h) PPC/PCO_2PU2(80/20), (i,j) PPC/PCO_2PU2 (80/30)

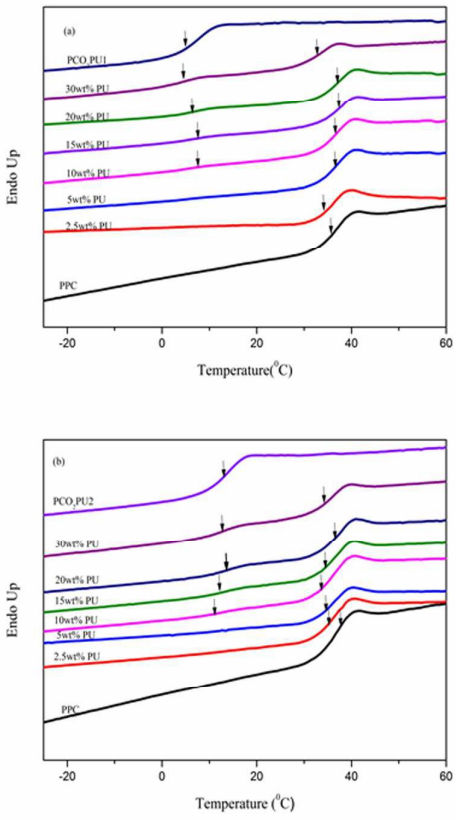

Fig. 4. DSC curves of PPC/PCO_2PUs with various PCO_2PU loadings: (a) PPC/PCO_2PU1, (b) PPC/PCO_2PU2

of obvious phase separation. The glass transition temperature of the miscible blend was between that of neat PPC and PU, which was a little higher than that calculated by the Fox equation. In immiscible blends composed of PPC and PCO_2PU1, the two glass transition temperatures displayed in all the blends were also between that of two components due to the diffusion of a mutually soluble T_g-reducing component from one phase to another. But interestingly, the lower T_gs in PPC/PCO_2PU2 blends corresponding to rubbery particle rich phase were lower than that of the PCO_2PU2. As reported in the PS/PE blends, the phenomenon may be owing to the interaction between the two components. [22]

3.4 Rheology analysis of various PPC/PCO_2PU blends

To confirm the miscibility of PPC and PCO_2PUs, rheology analysis has been conducted. Fig.S1. and Fig.S2. showed the dynamic frequency sweeps of PPC and PPC/PCO_2PU blends with various compositions. All the blends exhibited a decrease in viscosity with increase of frequency, indicating an obvious shear thinning behavior and the pseudoplastic characteristic. Meanwhile, the addition of PCO_2PU decreased the viscosity of PPC, which may favor the processability.

Due to the sensitivity of dynamic rheology to the change of morphology, it is generally used to study the miscibility of the blend. For homopolymer or miscible blends, when the frequency is small enough, the slope of log G' vs. log ω is 2, and the slope of log G'' vs. log ω is 1.[23] When phase separation occurs, the slope becomes smaller due to the contribution of elasticity of the interface, and the time-temperature superposition fails. For the PPC/PCO_2PU blends with various compositions, the plots of log G' vs. log ω were displayed in Fig. 5. As the content of PCO_2PU increased，the slope of log G' vs. log ω decreased gradually. When the loadings of two kinds of PCO_2PUs were 5 wt%, the slope was very close to 2, indicating the miscibility of the blends. With the loading increased to 10 wt%, the slope decreased to 1.78 and 1.68 for PPC/PCO_2PU1 and PPC/PCO_2PU2, respectively. The slope further decreased when PCO_2PU loading was 30 wt%. Therefore, the blends became immiscible with two kinds of PCO_2PUs loading above 10 wt%, which was in accordance with the DSC analysis. The different toughing effect of PPC/PCO_2PU blends may related with the phase morphology and was studied in section 3.5.

3.5 Phase morphology

Phase morphology is of vital importance to the toughening effect. The size[24] and its distribution, and even the shape of distribution phase[25] decide the microstructure formed during the impact process, thereby influence the value of impact strength. For cavitation observed initially at 20 wt% PCO_2PU1 loading, the phase morphologies of PPC/PCO_2PU blends under 20wt% PCO_2PU loadings were studied and the diameters of

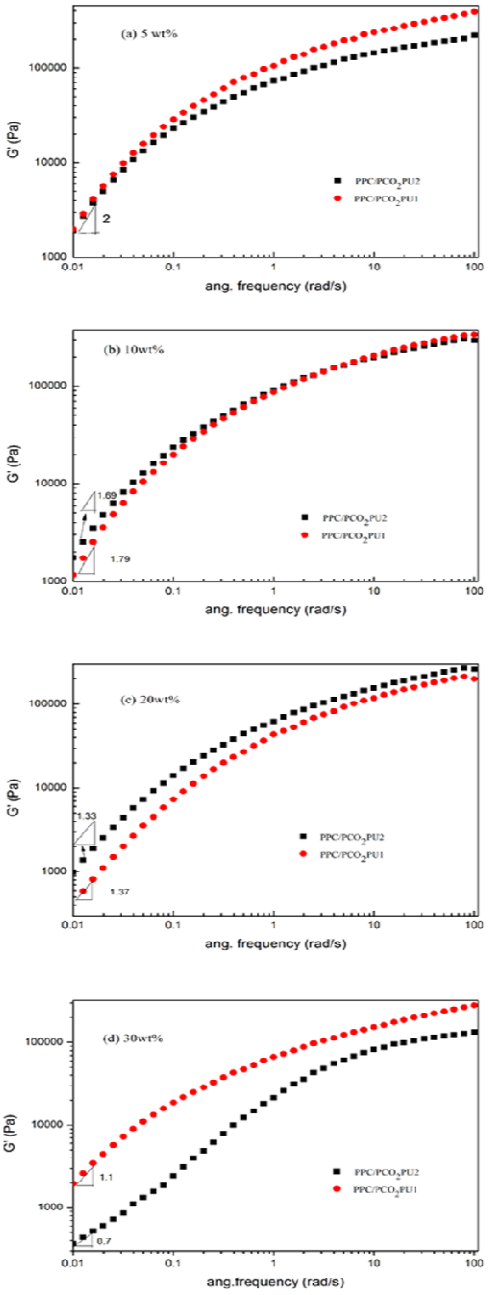

Fig. 5. G' of PPC/PCO_2PUs with various compositions at 1% strains. (a) 5 wt%, (b) 10 wt%, (c) 20 wt%, (d) 30wt%

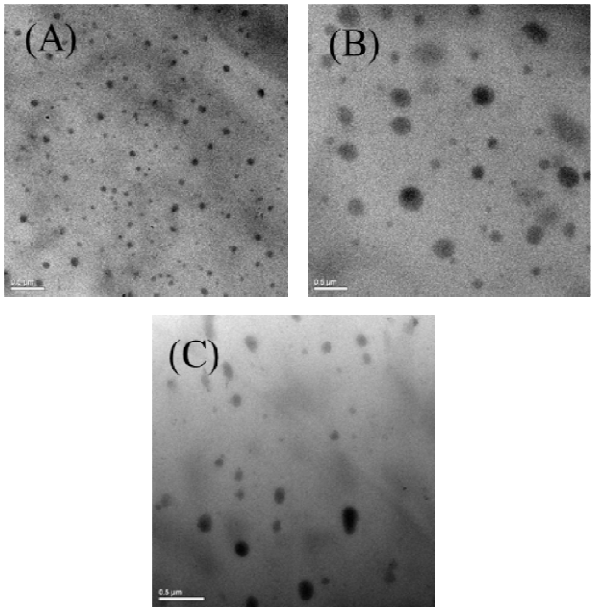

Fig. 6. Phase morphologies of PPC/PCO_2PUs with various compositions (A) PPC/PCO_2PU1 (85/15), (B) PPC/PCO_2PU1 (80/20), (C) PPC/PCO_2PU2 (80/20)

dispersed phase were displayed in Table S1 and Fig.6. As shown in Fig. 6, PCO_2PU was dispersed uniformly as spherical particles in PPC matrix in all the blends. When the content of PCO_2PU1 increased from 15 wt% to 20 wt%, the weight average diameter increased from 0.09 μm to 0.20 μm. While for the blend with PCO_2PU2 content of 20 wt%, the weight average diameter of dispersed phase was 0.11 μm, which indicated the PCO_2PU2 had better miscibility with PPC because of larger carbonate content. However, it seemed that the impact strength can be increased when the diameter of dispersed phase was as large as 0.20 μm, while the dispersed phase whose diameter was around 0.10 μm had nearly no contribution to the impact strength. Similar phenomenon was observed in PLA blends, where optimum particle size for increase of toughness was between 0.5-0.9 μm.[26] In PLA/P(CL-co-LA) blend, the observed particle size was 0.70 μm, the impact strength increased to 2 times of neat PLA.[25a] According to the theory developed by Paul,[12b] the shear yielding of the matrix occurs when the stress reaches the critical value, which is influenced by the cavitation of the dispersed phase. When the diameter of the rubber phase is too small to form the microvoids, the critical stress at the onset of shear yielding is so large that the strain energy release rate is sufficient to initiate crazing and crack growth in the plane strain region. As a result, the development of shear yielding is limited and fracture occurs first. It is noteworthy that the resistance of cavitation is related to the diameter of rubber phase, *i.e.*, the critical volume strain at cavitation increase as the diameter reduce. Therefore, there is a critical diameter beyond which the cavitation occurs before shear yielding. The cavitation favors the shear yielding by reducing the critical value at which shear yielding happens. As a result, energy dissipation is promoted and the impact strength increases.

In the PPC/PCO_2PU blends, the diameter of dispersed phase was believed to be a determining factor in these PPC/PU blends. The cavitation was found in the PPC/PCO_2PU1 (80/20) blend, in which the diameter of dispersed phase reached 0.20 μm, and shear yielding occurred with energy dissipated during the process of impact. While in other blends, the small diameter of dispersed phase led to the absence of microvoid, unstable crazes propagated before the shear yielding occurred. As a result, the notched impact strength increased little. The smaller toughening efficiency of PCO_2PU2 can be explained well, that is, better miscibility of PCO_2PU2 with PPC result in much smaller diameter of dispersed phase, which was unfavorable for the occurrence of cavitation.

4. Conclusion

Polyurethane containing carbonate unit was synthesized and used to toughen PPC thanks to their potential miscibility. Both the elongation at break and the tensile strength can be improved, and simultaneous reinforcement and toughening were realized. The notched impact strength of PPC was improved to 228.3 J/m for the first time, which was comparable to traditional bisphenol A polycarbonate. It was found that the increase of impact strength was related to the diameter of dispersed phase. When the diameter of dispersed phase reached 0.20 um, cavitation and matrix yielding occurred, which led to dissipation of energy and ductile fracture. Our research was helpful to understand the relationship between morphology and toughness and determine the range of efficient diameter of rubber phase in the area of toughening PPC.

Acknowledgments

The work was financially supported by the National Natural Science Foundation of China (Grant No. 51321062 and No. 21134002).

Notes and References

[a] Key Laboratory of Polymer Ecomaterials, Changchun Institute of Applied Chemistry, Chinese Academy of Sciences, Changchun 130022, People's Republic of China.
[b] University of Chinese Academy of Sciences, Beijing 100039, People's Republic of China
* CORRESPONDING AUTHOR: Dr. Yusheng Qin
Fax: +86 431 85262252; Tel: +86 431 85262252; E-mail: ysqin@ciac.ac.cn
** CORRESPONDING AUTHOR: Prof. Xianhong Wang
Fax: +86 431 85689095; Tel: +86 431 85262250; E-mail: xhwang@ciac.ac.cn

1. (a) D. J. Darensbourg, *Chem. Rev.*, 2007**, 107**, 2388; (b) S. Klaus, M. W. Lehenmeier, C. E. Anderson and B. Rieger, *Coordin. Chem. Rev.*, 2011**, 255**, 1460; (c) T. Sakakura, J.-C. Choi and H. Yasuda, *Chem. Rev.*, 2007**, 107**, 2365.
2. (a) N. Nagiah, G. Ramanathan, T. S. Uma, L. Madhavi, R. Anitha and T. S. Natarajan, *Adv. Polym. Technol.*, 2013**, 32**; (b) A. Welle, M. Kroeger, M. Doering, K. Niederer, E. Pindel and I. S. Chronakis, *Biomaterials*, 2007**, 28**, 2211.
3. Q. Lu, Y. Gao, Q. Zhao, J. Li, X. Wang and F. Wang, *J. Power Sources*, 2013**, 242**, 677.
4. F. Gao, Q. Zhou, Y. Dong, Y. Qin, X. Wang, X. Zhao and F. Wang, *J. Polym. Res.*, 2012**, 19**.
5. (a) Z. Bartczak, A. S. Argon, R. E. Cohen and M. Weinberg, *Polymer*, 1999**, 40**, 2331; (b) Q. Yuan, W. Jiang, H. Zhang, J. Yin, L. An and R. K. Y. Li, *J. Polym. Sci. Part B: Polym. Phys.*, 2001**, 39**, 1855.
6. (a) G. Gao, J. Zhang, H. Yang, C. Zhou and H. Zhang, *Polym. Int.*, 2006**, 55**, 1215; (b) L. D. Zhu, H. Y. Yang, G. Di Cai, C. Zhou, G. F. Wu, M. Y. Zhang, G. H. Gao and H. X. Zhang, *J. Appl. Polym. Sci.*, 2013**, 129**, 224.
7. Q. Zhou, F. Gao, X. Wang, X. Zhao and F. Wang, *Acta Polym. Sin.*, 2009, 227.
8. L. Chen, Y. Qin, X. Wang, X. Zhao and F. Wang, *Polymer*, 2011**, 52**, 4873.
9. L. Chen, Y. Qin, X. Wang, Y. Li, X. Zhao and F. Wang, *Polym Int.*, 2011**, 60**, 1697.
10. (a) J. J. Huang, H. Keskkula and D. R. Paul, *Polymer*, 2004**, 45**, 4203; (b) S. H. Wu, *Polymer*, 1985**, 26**, 1855; (c) S. H. Wu, *J. Appl. Polym. Sci.*, 1988**, 35**, 549; (d) Z. Z. Yu, Y. C. Ke, Y. C. Ou and G. H. Hu, *J. Appl. Polym. Sci.*, 2000**, 76**, 1285; (e) B. Majumdar, H. Keskkula and D. R. Paul, *J. Polym Sci. Part B-Polym Phys.*, 1994**, 32**, 2127.
11. (a) A. M. Donald and E. J. Kramer, *J. Appl. Polym. Sci.*, 1982**, 27**, 3729; (b) D. G. Gilbert and A. M. Donald, *J. Mater. Sci.*, 1986**, 21**, 1819; (c) M. Matsuo, T. T. Wang and T. K. Kwei, *J. Polym. Sci. Part a-2-Polym. Phys.*, 1972**, 10**, 1085; (d) J. C. Stendahl, E. R. Zubarev, M. S. Arnold, M. C. Hersam, H. J. Sue and S. I. Stupp, *Adv. Funct. Mater.*, 2005**, 15**, 487.
12. (a) C. B. Bucknall and D. R. Paul, *Polymer*, 2013**, 54**, 320; (b) C. B. Bucknall and D. R. Paul, *Polymer*, 2009**, 50**, 5539.
13. Y. Gao, L. Gu, Y. Qin, X. Wang and F. Wang, *J. Polym. Sci. Part a-Polym. Chem.*, 2012**, 50**, 5177.
14. (a) I. Kim, M. J. Yi, K. J. Lee, D. W. Park, B. U. Kim and C. S. Ha, *Catal. Today*, 2006**, 111**, 292; (b) B. Y. Liu, X. J. Zhao, X. H. Wang and F. S. Wang, *Polymer*, 2003**, 44**, 1803.
15. Y. Lin, K.-Y. Zhang, Z.-M. Dong, L.-S. Dong and Y.-S. Li, *Macromolecules*, 2007**, 40**, 6257.
16. J. J. Huang, H. Keskkula and D. R. Paul, *Polymer*, 2006**, 47**, 639.
17. (a) S. Balakrishnan and N. R. Neelakantan, *Polym. Int.*, 1998**, 45**, 347; (b) X. Zhi, H.-B. Zhang, Y.-F. Liao, Q.-H. Hu, C.-X. Gui and Z.-Z. Yu, *Carbon*, 2015**, 82**, 195.
18. S. B. N. Irvin Wolock, *Fracture Processes in Polymeric Solids: Phenomena and theory*, John Wiley & Sons Inc New York, 1964.
19. (a) G. M. Kim and G. H. Michler, *Polymer*, 1998**, 39**, 5689; (b) G. M. Kim and G. H. Michler, *Polymer*, 1998**, 39**, 5699.
20. H. Kang, B. Qiao, R. Wang, Z. Wang, L. Zhang, J. Ma and P. Coates, *Polymer*, 2013**, 54**, 2450.
21. C. Geng, J. Su, S. Han, K. Wang and Q. Fu, *Polymer*, 2013**, 54**, 3392.
22. V. Thirtha, R. Lehman and T. Nosker, *Polymer*, 2006**, 47**, 5392.
23. J. D. Ferry, *viscoelastic properties of polymers*, Wiley, New York, 1980.
24. Y.-S. He, J.-B. Zeng, G.-C. Liu, Q.-T. Li and Y.-Z. Wang, *RSC Adv.*, 2014**, 4**, 12857.
25. (a) J. Odent, P. Leclere, J.-M. Raquez and P. Dubois, *Eur. Polym. J.*, 2013**, 49**, 914; (b) H. Xiu, C. Huang, H. Bai, J. Jiang, F. Chen, H. Deng, K. Wang, Q. Zhang and Q. Fu, *Polymer*, 2014**, 55**, 1593.
26. (a) G. C. Liu, Y. S. He, J. B. Zeng, Y. Xu and Y. Z. Wang, *Polym. Chem.*, 2014**, 5**, 2530; (b) W. M. Gramlich, M. L. Robertson and M. A. Hillmyer, *Macromolecules*, 2010**, 43**, 2313.